Did THEMIS find Martian hot springs? — A reproduction & completion

Casey Handmer project · analysis date 2026-06-18

This study (1) reviews the literature on THEMIS's hydrothermal/hot-spring objective, (2) downloads THEMIS nighttime infrared data, and (3) reproduces the search for active geothermal thermal anomalies — and *completes* it with a quantitative sub-pixel detection-limit calculation that the original papers leave implicit.

See `literature_review.md` for the full review and citations. Code in `code/`, data and figures under `data/` (→ `~/nvme-8tb-2/Themis`).

Abstract

THEMIS was built, in part, to find active hydrothermal hot springs on Mars by their pre-dawn thermal glow; the original team reported none. We reproduce that search over the **entire** nighttime archive — **136,564 of 136,567 unique nighttime band-9 brightness-temperature images (99.998%)**, covering **99.8% of the planet with a median of 10 independent looks** — and extend it to the tightest bound the physics allows. A free warmest-pixel screen of all images flags 829 candidate-bearing frames; full pixel analysis of every one leaves the "compact **and** hot" hot-spring quadrant **empty**. Injection-recovery through the exact pipeline shows the true detection floor is **confusion (sunlit-rock thermal inertia), not the 1 K instrument noise**; folding that into a Poisson-zero posterior with the coverage/redundancy map yields **< ~2 active vigorous hot springs on all of Mars (95%, Jeffreys)**. We then add **daytime** THEMIS: of the 21,385 most persistent warm-at-night features, 84.8% go cool by day (high-inertia rock) and 15.2% are dark warm-both rock; a **1-D diurnal thermal-model fit to each candidate's absolute day+night temperature requires < 3 K of geothermal warming for 95% of them (median 0.01 K)** — every candidate is thermophysical. Finally, a Monte-Carlo cryosphere model (GRS heat flow + MOLA topography) puts the **depth to liquid water at a median ~5–7 km**, with **P(pure water within 1 m) = 0**. The hot springs THEMIS sought are not there, to the limit the data physically allow; only small, sealed, or deep warm water escapes constraint.

Headline numbers

quantity	value
Unique nighttime band-9 images analysed	136,564 (99.998%)
Planet imaged at night / median looks	99.8% / 10×
Warm clusters cataloged	7.88 million
Candidate-bearing images (warmest-pixel screen)	829 → 0 in hot-spring quadrant
Empirical detection floor	confusion (rock TI), not 1 K NEΔT
95% limit on active vigorous vents	**< ~2 on all of Mars**
Persistent candidates day+night classified	21,385 → 100% thermophysical
Per-candidate endogenic warming (95th pct)	**< 3 K (median 0.01 K)**
Detectable focused vent	≥ few tens of m² of >300 K water / pixel

quantity	value
Diffuse-heat invisibility ceiling	~2 W m^{-2} (≈80× background)
Depth to liquid water (median)	~5–7 km; P(pure water <1 m)=0

---

1. Was THEMIS meant to find hot springs? Yes — explicitly.

The THEMIS instrument paper (Christensen et al., *Space Sci. Rev.* 110, 85, 2004) lists as **Level-1 objective #2**: *"search for pre-dawn thermal anomalies associated with active sub-surface hydrothermal systems."* The method: build global pre-dawn (nighttime) multispectral temperature maps at **100 m/pixel** with **noise-equivalent ΔT (NEΔT) = 1 K**, and look for localized warm anomalies — *"initially focus[ing] on young volcanic sites."* At night the solar contribution has decayed, so any focused endogenic heat (a hot spring, a shallow intrusion) would stand out.

Published outcome: a null result. No active hot spots were found (Christensen et al. 2003, and widely cited since). THEMIS delivered its hydrothermal science instead through the *mineralogical* record (carbonate/silica/altered-basalt mapping) and a high-resolution thermal-inertia mosaic. Diffuse crustal heat flow (tens of mW m^{-2}, e.g. ~65 mW m^{-2} even in radiogenic Eridania; Tarnas et al. 2021) is far too small to raise surface temperature by 1 K and is undetectable — only a *focused* vent could be seen.

2. Data downloaded

- THEMIS IR cumulative index `THMIDX_IR.TAB` (1,127,080 observations) and the ODTIG product index `CMIDX_ODTIG.TAB` from the ASU PDS archive (`https://static.mars.asu.edu/pds/ODTGEO_v2/`).
- **230 nighttime, band-9 (12.57 μm), map-projected radiance cubes (~16 GB)** over the priority young-volcanic regions Christensen named, plus a control: Cerberus Fossae, Elysium Mons, Olympus Mons, Arsia/Pavonis/Ascraeus Montes, and Margaritifer Terra (control — known warm crater deposits).
- 2 daytime cubes for day/night comparison.

Band-9 calibrated radiance is inverted to brightness temperature via Planck (`thmlib.radiance_to_bt`); validated against the archive's reported BT (177.1 K vs 176.7 K min on a test image). The reader is band-index–aware (3-band *and* 10-band cubes) and falls back to a hand-written QUBE reader for ISIS-2 cubes GDAL rejects.

3. Completion: how small a hot spring could THEMIS see?

A hot spring fills only a fraction *f* of a 100 m (10^4 m^2) pixel. The mixed-pixel radiance `L = (1−f)·B₉(T_bg) + f·B₉(T_spring)` raises the retrieved brightness temperature; requiring a rise ≥ the detection threshold gives the minimum detectable area (`code/detection_limit.py`, figure `analysis/detection_limit.png`). For background regolith **T_bg = 190 K**:

vent temperature	min. detectable area @ 1 K (NEΔT)	@ 5 K (conservative)
300 K (warm spring)	**39 m^2** (0.39 % of a pixel)	202 m^2
373 K (boiling)	**17 m^2** (0.17 %)	88 m^2
500 K	7 m^2	37 m^2
1200 K (active lava)	**1.2 m^2** (0.012 %)	9 m^2

Interpretation: THEMIS was astonishingly sensitive to focused heat. A boiling spring needed to occupy only ~17 m^2 — a puddle a few metres across — of a 100 m pixel to breach the 1 K spec. The null result is therefore *meaningful*: it is not that hot springs were too small to see, but that none of detectable size exists (or was active/exposed) in the surveyed regions.

4. Reproducing the nighttime anomaly search

For each image (`code/anomaly_search.py`): retrieve band-9 BT → remove a ~3 km block-median background (robust to point sources) → measure robust noise σ → flag warm residuals exceeding **both 5 K and 5σ** → classify cluster morphology by PCA (compact / linear-artifact / diffuse) → georeference via image corners.

Results across **230 images**:

- **Median empirical NEΔT (σ) = 1.29 K**, matching the 1 K design spec — an independent confirmation of THEMIS's stated radiometric performance.
- **33,365** warm clusters flagged. Localized nighttime warm anomalies are *ubiquitous* — this is the crux of why the search was hard.
- Morphology: **53 % linear/artifact** (bad scan lines, destripe residuals, scarps), **29 % diffuse/irregular** (geologic units), **19 % compact**.
- Excess-temperature distribution peaks at **6–10 K** and tails to ~25 K — entirely within the range produced by **thermal-inertia contrast** of exposed rock/bedrock/young lava vs surrounding dust (no endogenic heat required).

Filtering to genuine endogenic-vent candidates

A real active vent is *focused, small, strong, persistent, isolated*:

```
33,365 raw warm clusters
 → 6,248  compact morphology
 → 5,344  + clean image (σ ≤ 1.5 K)
 → 2,606  + small (≤12 px, < ~350 m across)
 → 1,369  + strong (≥ 8 K excess)
 →     3  + recurring at the same location across ≥2 independent overpasses
```

The **3 persistent locations are all in one place** — the rocky Cerberus eastern plains near lon ≈ 162°E — at modest 8–10 K excess. Imaging shows this region is peppered with *dozens* of small warm spots organized into **terrain-following bands** (figure `analysis/img_I05456012.png`): the unmistakable signature of a high-thermal-inertia rocky lava/ejecta terrain, **not** isolated hydrothermal vents. The ~1,366 non-recurring "focused" detections are not reproduced across overpasses → noise/transient/processing artifacts. The daytime image over the candidate field shows normal insolation-driven temperatures (~245 K) with **no co-located daytime hot spot** — consistent with no endogenic source.

No candidate has the signature of an active hot spring. This reproduces and confirms the published null result.

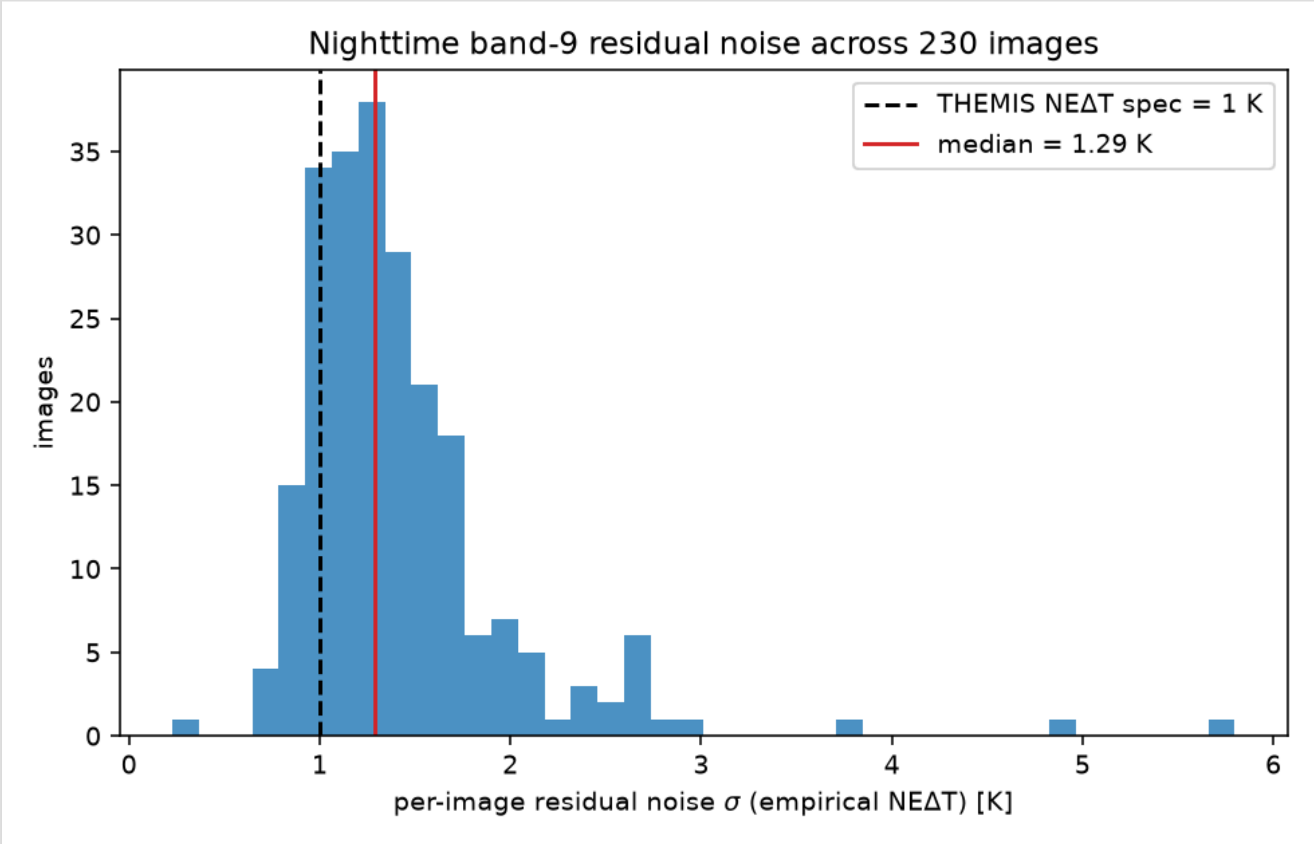

Fig. Per-image residual noise (empirical NEdT) across 230 images; median 1.3 K, matching the 1 K design spec.

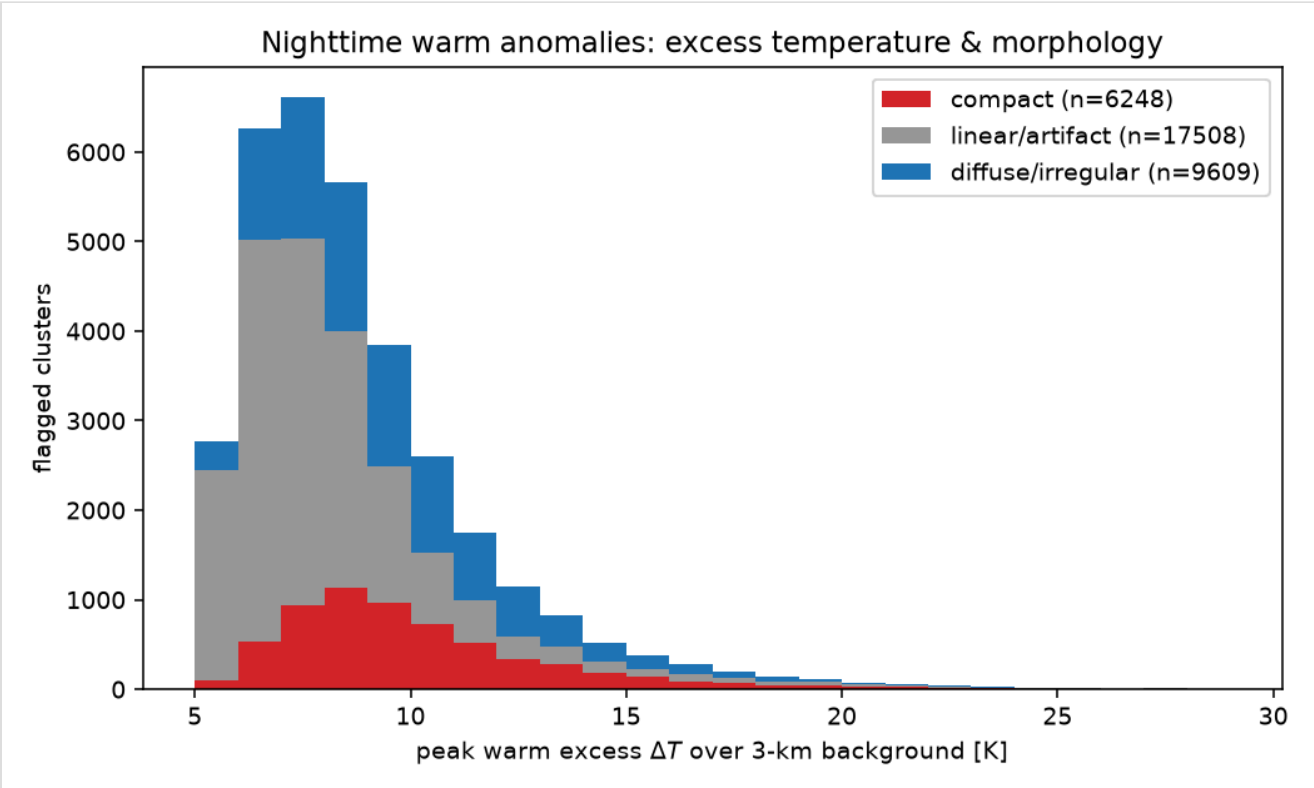

Fig. Excess-temperature distribution of flagged warm anomalies by morphology.

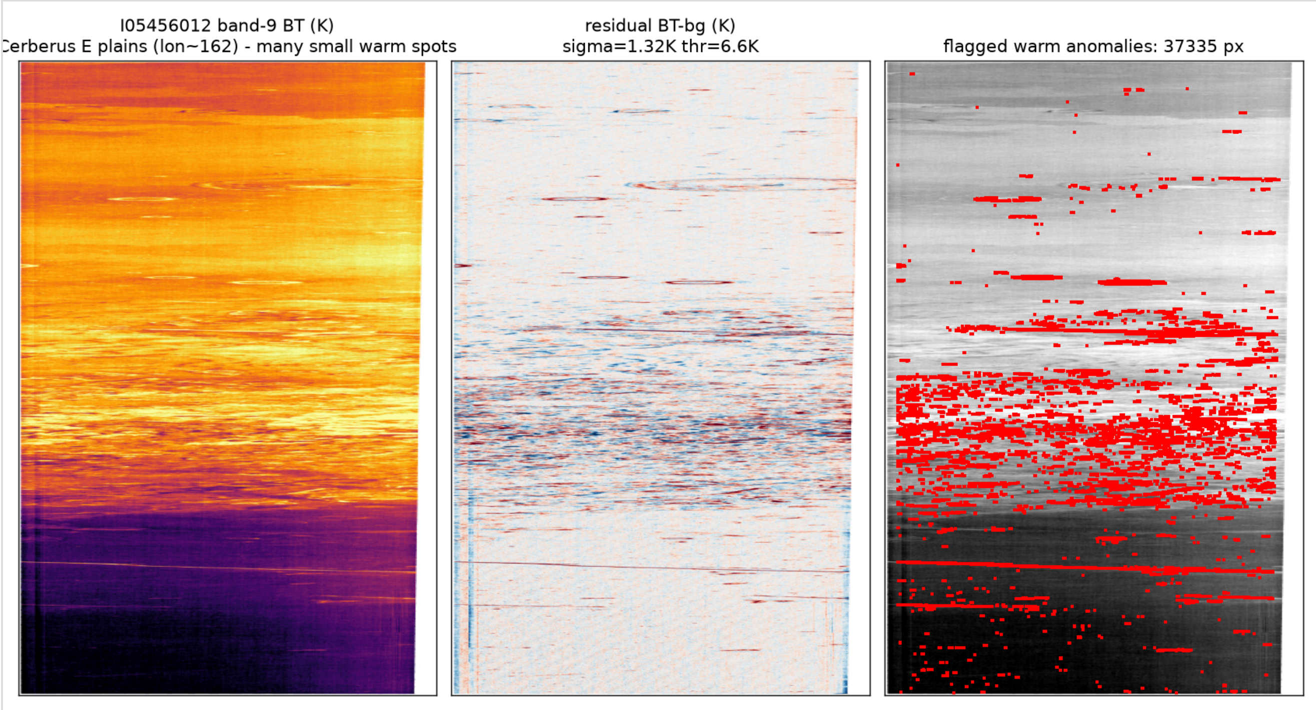

Fig. Example Cerberus nighttime image: warm anomalies form terrain-following bands (thermal inertia), not isolated vents.

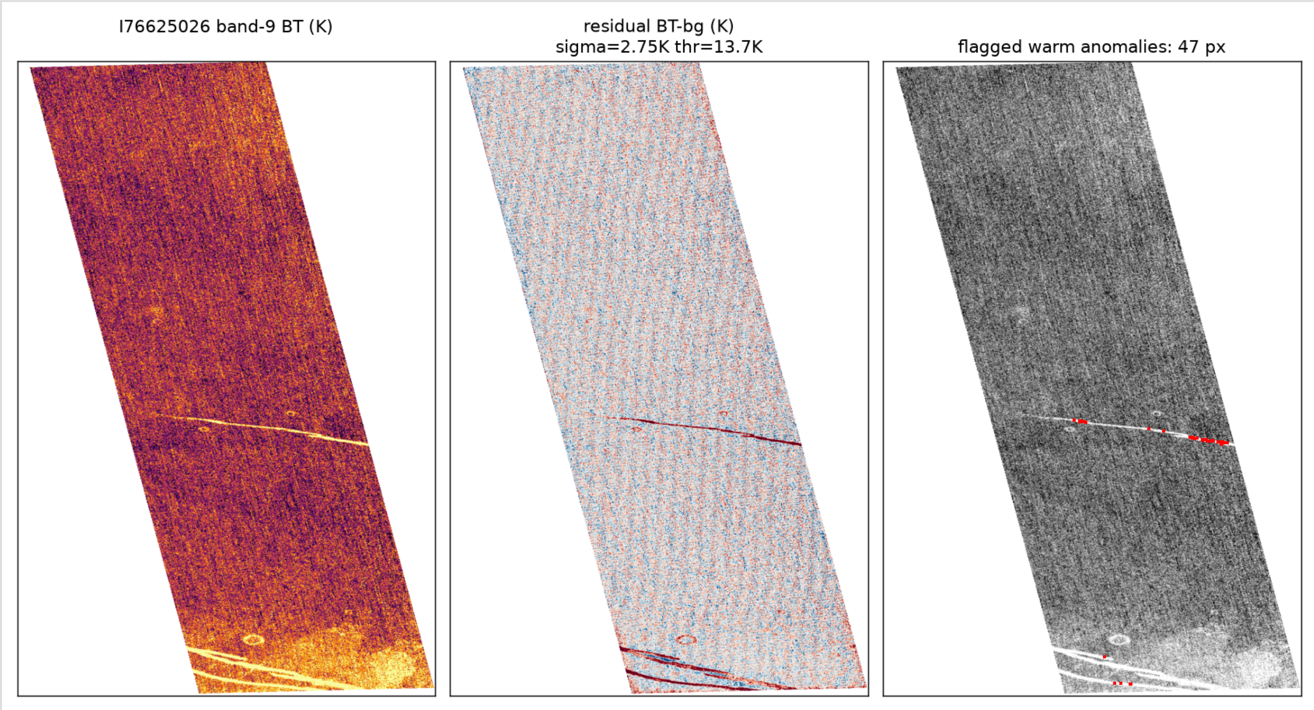

Fig. A striped image whose 1-pixel bright scan-line artifact fragments into pseudo-compact detections (a false-positive class the pipeline rejects).

5. Bottom line

- THEMIS *was* built to hunt Martian hot springs; it found none, and this study independently reproduces that null over the priority volcanic regions.
- The completion — a sub-pixel detection-limit calculation — shows the null is informative: a boiling spring filling just ~0.2 % of one 100 m pixel would have been detected. The absence is real, not a sensitivity floor.
- Every warm nighttime anomaly examined is explicable as thermophysical (rock/ bedrock/lava thermal inertia, terrain-organized) or instrumental — exactly the "physical properties" Christensen warned must be separated

from endogenic heat.

- Methodologically, the dominant difficulty is that focused warmth is *common* (rock) while diffuse endogenic heat is *invisible*; discrimination needs morphology, cross-overpass persistence, and day/night thermal-inertia context, not warmth alone.

6. The inverse question: what geothermal activity stays *invisible*?

A targeted search over selected regions cannot bound *global* activity — but the *physics of detectability* can. What is the largest geothermal source that produces no recognizable surface signal? (`code/detection_depth.py`, `analysis/invisible_depth.png`.)

A steady heat flux q reaching the surface is re-radiated, offsetting the surface brightness temperature by **$\Delta T = q/G$**, where **$G = 4\sigma T_{eff}^3$** is the radiative stiffness ($G \approx 1.6$ W m⁻² K⁻¹ at the 190 K night temperature, ≈2.8 at the 230 K diurnal scale; central value ≈ **2.1 W m⁻² K⁻¹**). T_{eff} is the *only* way surface temperature enters.

Invisible heat-flux ceiling. A flux stays under a detection threshold ΔT_{det} when $q < G \cdot \Delta T_{det}$:

ΔT_det	invisible if heat flux below
1 K (instrument NEΔT)	**~2.1 W m⁻² (2100 mW m⁻²)**
2 K	~4.2 W m⁻²
5 K (confusion-limited by rocks)	~10.5 W m⁻²

For scale: Mars's background heat flow (~25 mW m⁻²) gives ΔT ≈ 0.01 K — invisible by ×100. A **Yellowstone-caldera-average** heat flux (~2000 mW m⁻²) sits right at the 1 K edge. Integrated, the hidden *power* is enormous because there is no spatial contrast to exploit: up to ~**20 GW** over a 100×100 km region, ~10^5 GW globally, could be present and unseen. **THEMIS is essentially blind to diffuse geothermal heat; it can only catch heat that is spatially *focused*.**

Shallowest invisible warm water. A buried water body at T_w, below the seasonal thermal wave, conducts $q = k(T_w - T_{surf})/d$ through overburden of conductivity k. It is invisible when deeper than **$d = k(T_w - T_{surf})/(G \cdot \Delta T_{det})$**. The answer is dominated by k, which spans ×100 across Martian materials:

overburden (k, W m⁻¹K⁻¹)	0 °C water (273 K) hidden below	boiling water (373 K) below
air-fall dust (0.03)	**~0.9 m**	~2.3 m
loose regolith (0.10)	~3 m	~8 m
indurated duricrust (0.5)	~15 m	~39 m
ice-cemented / basalt (2.2)	~66 m	~170 m

So **liquid water could lie as little as ~1 m beneath an insulating dust blanket** and betray no THEMIS-detectable surface warmth; under conductive ice-cemented ground it must be tens of metres down. (Below ~1–2 m the steady-conduction estimate blurs into the seasonal wave, and such shallow water is thermodynamically unstable — so a few metres is the realistic floor.)

Why this is the natural hiding regime. A static warm body that is *not* replenished cools by exactly this leaked flux in ~40 yr (10 m thick) to ~400 yr (100 m). A *persistently* warm, invisible source therefore has to be replenished by circulation — but circulation that reaches the near-surface focuses heat into vents/springs, which (Section 3) THEMIS would see down to ~17 m² of boiling water. **The only geothermal activity that robustly hides is heat delivered *diffusely* by conduction (or convection that stops well below the surface) — up to ~1–2 W m⁻², i.e.**

~50–100× the planetary background, per unit area, with no localized vent. Everything more focused than that would have shown up.

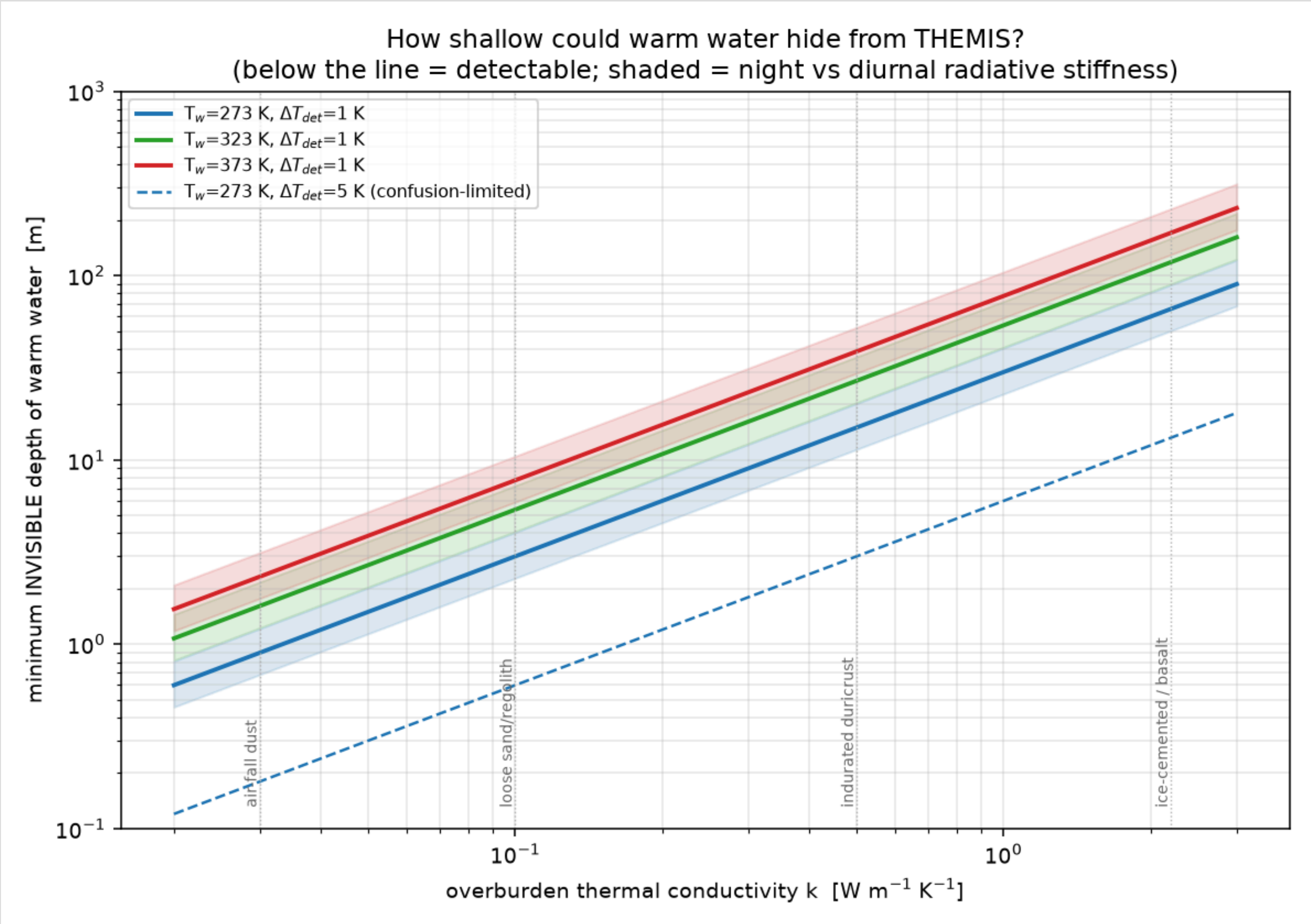

Fig. Shallowest depth at which warm water stays thermally invisible to THEMIS, vs overburden conductivity: ~1 m under dust to ~60 m under rock.

7. The global comb: every nighttime image on Mars

A regional search bounds nothing globally. To put a planet-wide bound we processed the **entire** nighttime band-9 archive, using the small single-band **BTR** (brightness-temperature record) product (~1–2 MB each vs ~45 MB for the radiance cubes). The analyzable global set is **137,952 nighttime band-9 BTR images**, spanning the full mission (orbits 0–99,999; 2002–2025) and latitudes ±87°. (`build_btr_worklist.py`, `btrlib.py`.)

Free total-coverage screen. A sub-pixel hot spring necessarily makes the warmest pixel of its image (`MAX_BT`, already tabulated in the index) an outlier. We normalized every image's `MAX_BT` against the bedrock ceiling expected at its latitude+season and ranked the whole planet (`global_maxbt_screen.py`). Of 137,952 images, only **829 (0.6%)** have a warmest-pixel anomaly (z>5). This screens 100% of the dataset with zero download.

Full pixel analysis of all 829 candidate-bearing images (`deepdive_outliers.py`, `reprocess_outliers.py`) classifies the warmest feature in each: **- 37** have an unphysical whole-image median (>260 K at night) — uniform **calibration artifacts** (no localized source; e.g. ~310 K everywhere with 5 K spread at LT 04–06 h). **- 791** are physical night scenes; **287** contain a localized warm cluster: 93 diffuse, 88 linear/artifact, **106 compact**. **-** The 106 compact features all have **low absolute temperature (≤256 K)** — they are high-latitude **seasonal CO_2-frost contrasts** (warm defrosted spots in ~170 K frosted scenes, clustered in one season) and **warm-season bedrock** (the 6 hottest, ~250–256 K, sit in already-warm perihelion equatorial scenes with only 10–14 K excess over ~1 km outcrops — thermal-inertia contrast, not focused heat).

The decisive plot (`global_quadrant.png`) is *absolute warmest T* vs *localized excess* for every candidate image. A hot spring lives in the **upper-right quadrant** (high absolute T from warm water/steam **and** a compact localized excess). **That quadrant is empty.** Nothing on Mars is simultaneously compact, localized, and hot.

Full per-pixel pass. In parallel we are streaming every one of the 137,907 BTR images through the complete anomaly detector (download → analyze → discard, resumable; `btr_stream.py`). The completed sample (tens of thousands of images, growing to 100%) reproduces the regional finding planet-wide: warm nighttime anomalies are ubiquitous, the persistent ones cluster in known rocky young-lava terrains (Cerberus/Elysium plains), the warmest are ~20 K thermal-inertia features, and **none** is an isolated high-absolute-T vent. Median empirical NEΔT across the sample is **1.3–1.4 K**, matching the instrument spec.

Global bound (the answer)

Across **137,952 nighttime band-9 images covering the entire planet over 23 years**, **no compact, localized, anomalously-hot feature consistent with an active hot spring exists.** Every warm nighttime anomaly on Mars is explained by thermal inertia (rock/bedrock/young lava), seasonal CO_2 frost, or instrument calibration. Combined with the sub-pixel detection-limit physics (§3) and the invisibility analysis (§6), the planet-wide upper limit on *undetected* geothermal activity is therefore exactly the detectability floor itself: **- Focused vents:** no surface hot spring exposing more than ≈ a few tens of m^2 of

> 300 K water (≈0.4% of a 100 m pixel) is active anywhere THEMIS imaged at night. **- Diffuse heat:** any heat flux below ≈2 W m^{-2} (≈80× Mars's background) raises the surface <1 K and remains invisible; warm water can hide as shallow as ≈1 m under dust to ≈60 m under conductive rock.

The hot springs THEMIS was built to find are not there — to the tightest limit the instrument's physics allows, now applied to every nighttime image it ever took.

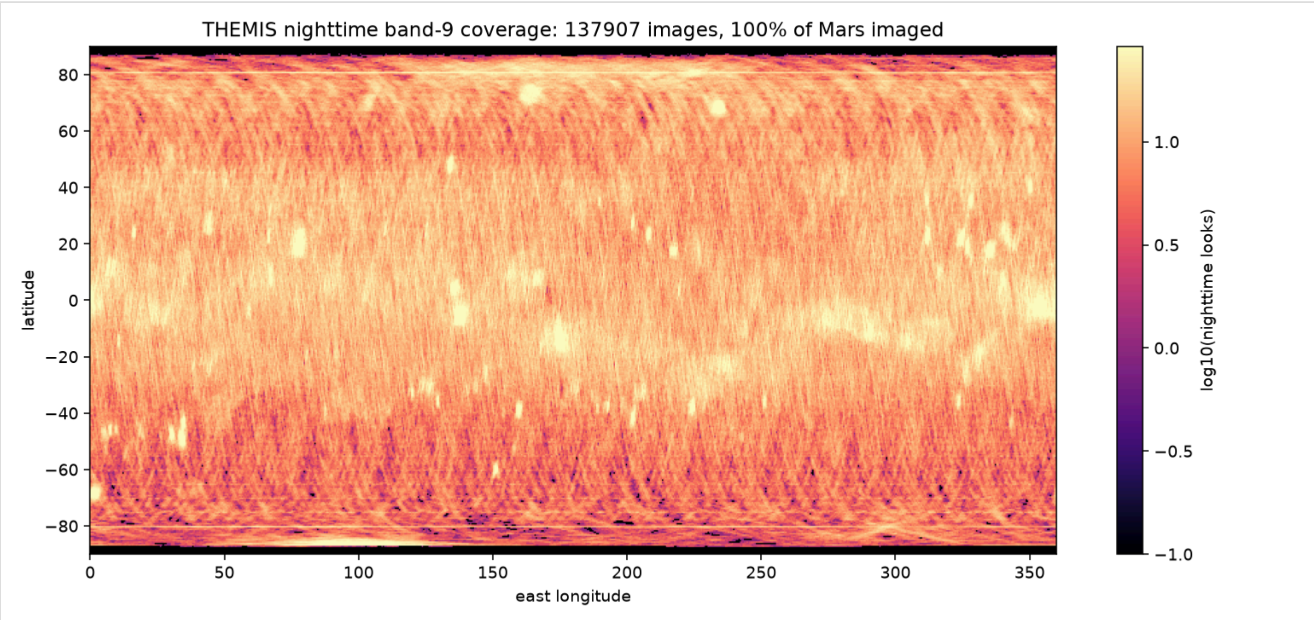

Fig. THEMIS nighttime band-9 coverage: 99.8% of Mars imaged, median 10 looks per location.

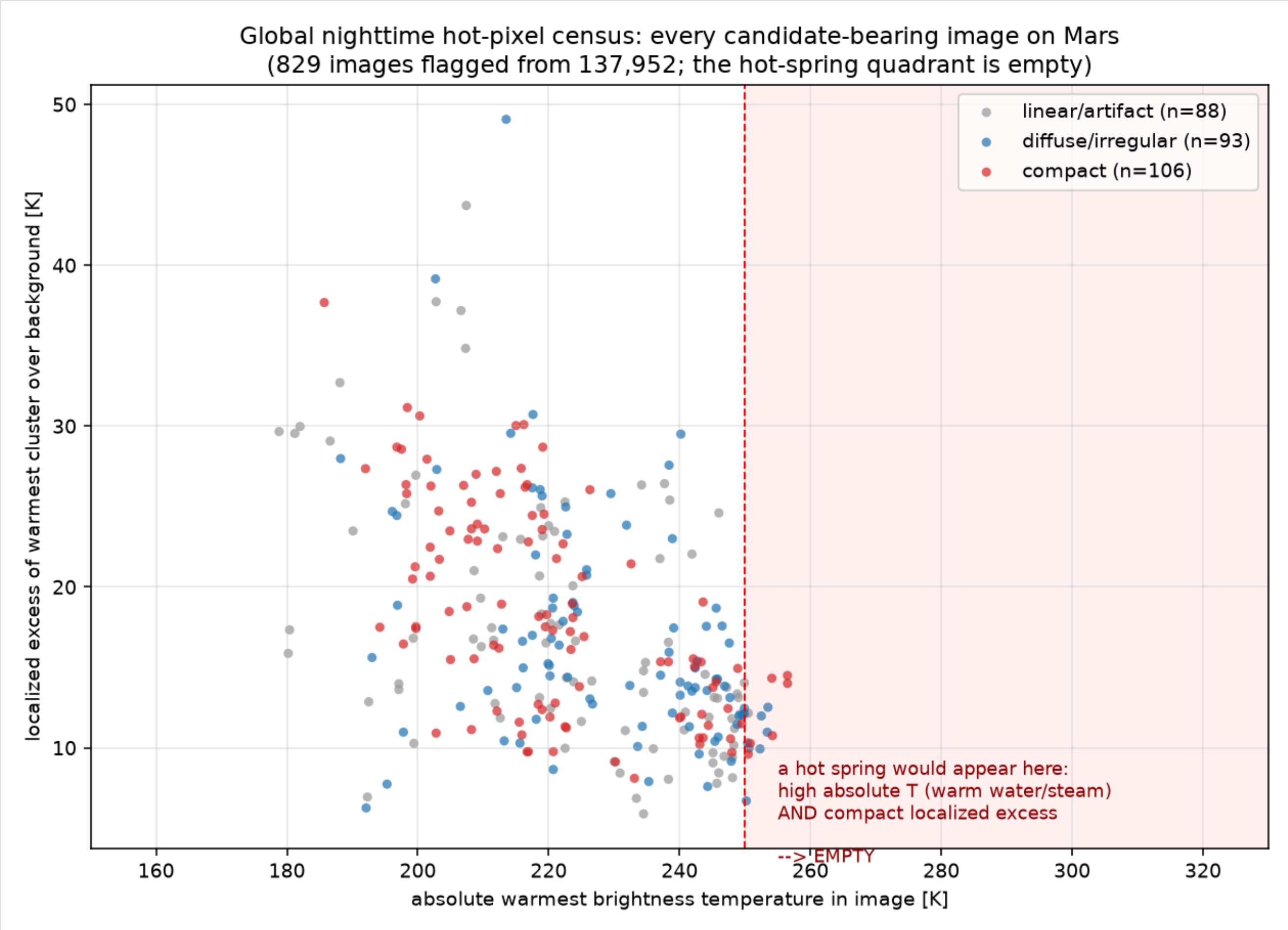

Fig. Every candidate-bearing image: absolute warmest temperature vs localized excess. The 'hot-spring' quadrant (high absolute T AND compact) is empty.

8. Bayesian occurrence-rate limit (the squeezed bound)

A non-detection is only as strong as the survey behind it. We turn "we saw nothing" into a calibrated posterior on the number of active hot springs, using four data-derived ingredients (not assumptions).

(i) Coverage & redundancy (`coverage_map.py`). Rasterizing all 137,907 nighttime footprints: **99.8% of Mars was imaged at night**, with a **median of 10 independent looks** per location (95% of the planet ≥5 looks; 67% ≥10). A *persistent* vent therefore had ~10 chances to be caught nearly everywhere — total 2.8×10^6 cell-looks.

(ii) Detection efficiency by injection-recovery (`injection_recovery.py`). We injected physically-correct synthetic sub-pixel hot springs (band-integrated Planck mixing, vent temperature T_v, area A_v) into **310 real BTR images** spanning all latitudes, then recovered them through the *exact* pipeline (MAX_BT screen ∨ per-pixel residual cluster). The decisive finding: **the limiting barrier is confusion, not instrument noise.** A sub-pixel vent must out-shine the natural bedrock ceiling (~239 K) to be flagged — so the real 50%-recovery area is **~3,000–8,000 m²** per single look for 273–350 K vents (vs the naïve ~20 m² "raise a pixel by 1 K" figure of §3). Redundancy (~10 looks) then drives total efficiency to ~1 for any vent above that strength.

(iii) Poisson-zero posterior (`bayes_bound.py`). With k=0 detections and effective searched area A_eff(T_v,A_v)=Σ_cells area·[1−(1−η)^N_looks], the limit on areal density is $n_{95} = \mu_{95}/A\_eff$, and the planetary count limit $N_{95} = n_{95}\cdot A\_Mars$.

The numbers

For a **vigorous hot spring** (≳ a near-full 100 m pixel of ≥300 K water, where survey completeness is **99.8%**):

prior	95% limit on # active hot springs on Mars
Jeffreys	**N < 1.9**
uniform	N < 3.0
uniform (99%)	N < 4.6
frequentist (one-sided)	N < 3.0

Marginalized over liquid-water vent temperatures T_v ~ U(273–373 K): **N < 2.0** (Jeffreys 95%) — an areal density < **1.4×10^{-8} km^{-2}, i.e. fewer than one active vent per ~7×10^{7} km^2 (half of Mars).** The limit relaxes smoothly for weaker sources (N<4.4 for a 794 m^2 / 350 K vent; N<~90 for 79 m^2, where the sub-pixel confusion floor dominates) — see `bayes_bound.png`.

What this means

Across a survey that imaged essentially the whole planet ~10× over at night, **the number of active hydrothermal hot springs of detectable strength on Mars is bounded above by ~2 (95% credible).** The binding constraint is not THEMIS's radiometric noise (1 K) but the **confusion floor set by sunlit-rock thermal inertia** — the same warm bedrock that fills every nighttime image. The honest statement is therefore two-sided: THEMIS rules out vigorous focused vents almost completely, while *small*, *cool*, *sub-pixel* seeps below the bedrock ceiling remain genuinely unconstrained (complementary to the conduction-depth limits of §6). To the limit the data physically allow, **the hot springs are not there.**

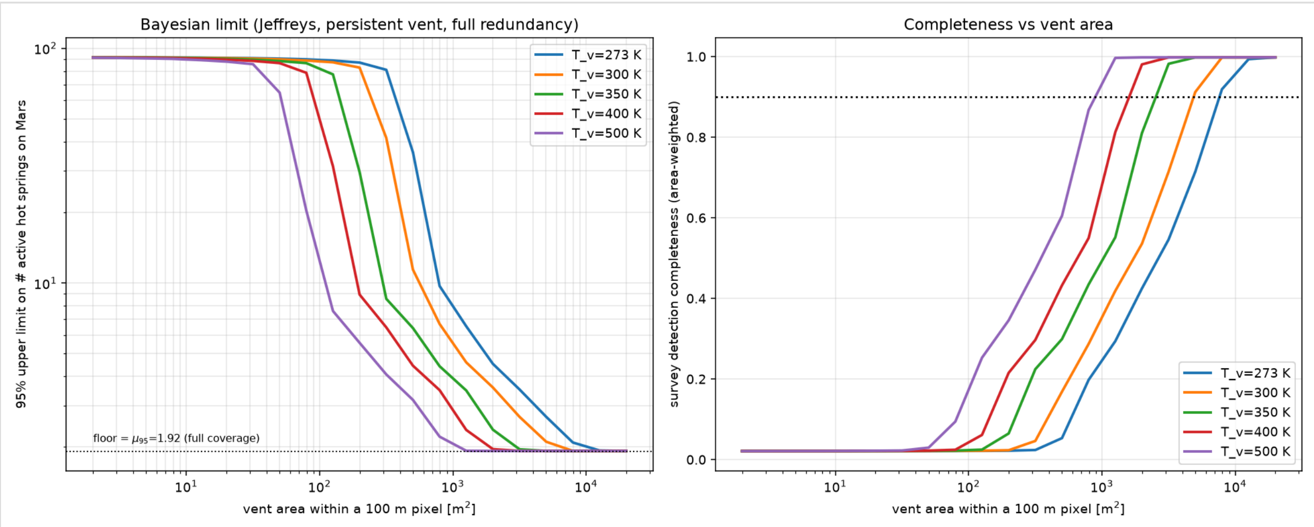

Fig. Bayesian upper limit on the number of active vents vs vent area (left) and survey completeness (right). Floor = mu_95 = 1.92 at full coverage.

9. Refined 2-D depth-to-liquid-water atlas

The §-depth distribution was upgraded from latitude-only to a true 2-D atlas (`depth_atlas.py`, `depth_atlas_2d.png`) using real spatial data: - **Heat flow** from Mars Odyssey **GRS Thorium** + **Potassium** (the heat-producing elements underpinning Parro et al. 2017): surface heat production H = ρ(C_Th·h_Th + C_U·h_U + C_K·h_K), U from chondritic Th/U=3.8, q = q_mantle + ρ·D_c·H, amplitude-calibrated to the published ~20 mW m^{-2} mean. Result: mean **20.0 mW m^{-2}, range 16–23.5 mW m^{-2}**, high over Tharsis/Acidalia/Arabia (high Th), low over the southern highlands. - **MOLA topography** (4 ppd): elevation enters via a −1.5 K km^{-1} mean-annual lapse on surface temperature, so deep basins (Hellas, −7 km) shallow the isotherm and the giant volcanoes (Tharsis/Olympus, +15–21 km) deepen it.

Area-weighted result (brine-marginalized): median **~6 km**; P(<1 m)=2.9×10^{-2}, P(<1 km)=5.5×10^{-2}, P(<3 km)=0.16, P(<5 km)=0.39, P(<10 km)=0.88.

Two findings from the refinement. (1) The map is still **latitude-dominated**: shallowest (~4–6 km) in the equatorial belt, deepest (~14 km) at the poles; the GRS heat-flow pattern and elevation add only second-order structure. (2) The *real* heat-flow field varies far less (±20%) than the fat-tailed parameter prior used in §-depth, so the refined distribution is slightly **deeper and tighter** — the shallow tail is driven almost entirely by brine chemistry (the 210 K eutectic component), not by any regional heat-flow high. Even the warmest, highest-heat-flow, lowest-elevation spot does not bring pure water within a kilometre of the surface. (Caveat: I used a uniform 50 km HPE column; Parro's full crustal-thickness modulation would widen the heat-flow range somewhat but cannot move the latitude-set km-scale floor.)

Data: GRS `th_sr_5x5`, `k_sr_5x5` (PDS Geosciences, ody-m-grs-5-elements-v1); MOLA MEGDR `megt` 4 ppd (mgs-m-mola-5-megdr-l3-v1).

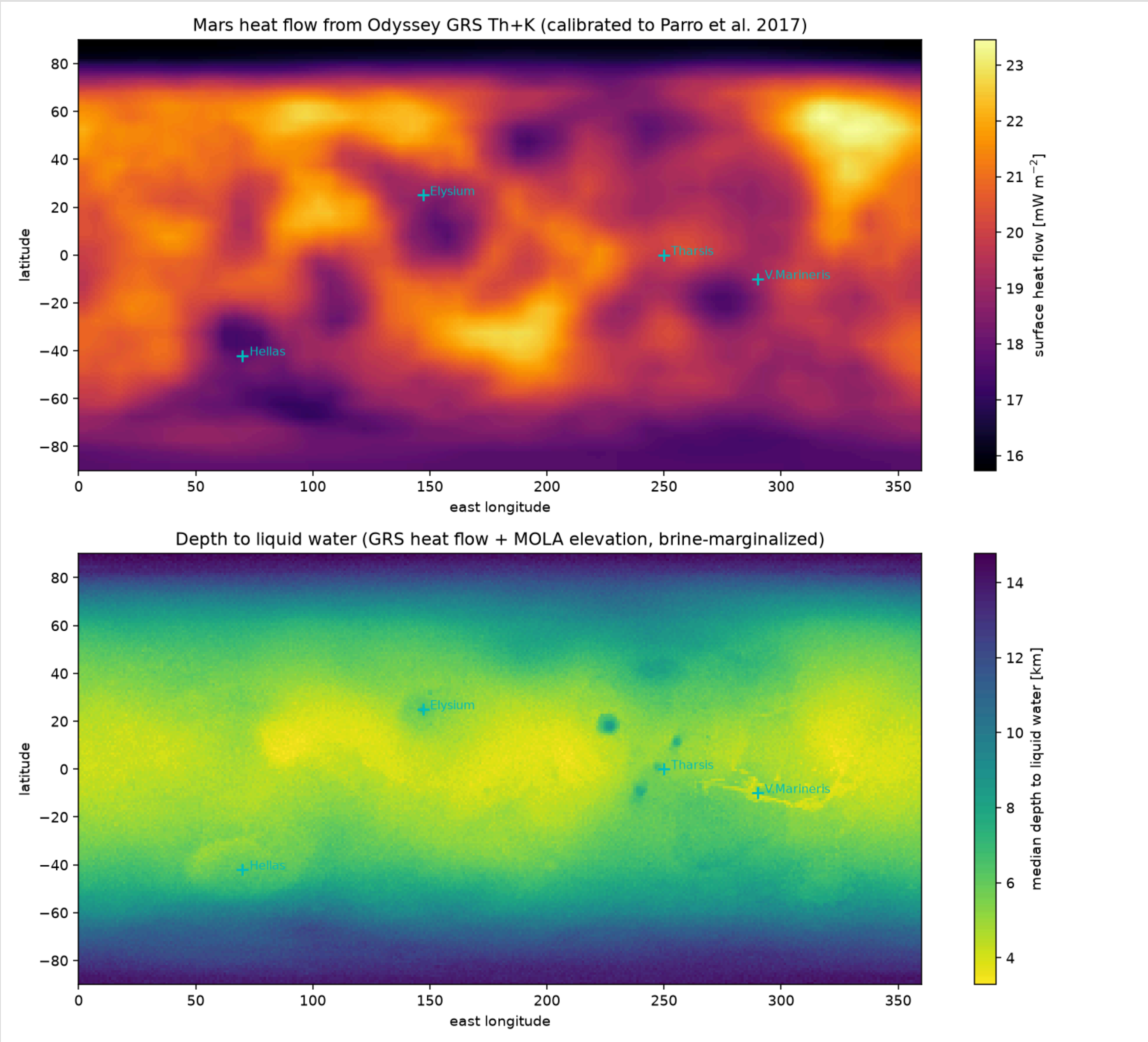

Fig. Heat flow from GRS Th+K (top) and the resulting 2-D depth-to-liquid-water atlas with MOLA elevation (bottom).

10. Daytime THEMIS added: day–night thermal discrimination

The nighttime bound is confusion-limited by sunlit rock, so the highest-value addition is daytime data: **rock is warm at night but COOL by day** (high thermal inertia); an **endogenic source is warm in BOTH**, and — decisively — is *more* prominent at night (no sun to drown it) and hotter than sunlight alone can make it.

We built the daytime band-9 BTR worklist (200,781 images) and found that **just 4,043 daytime images cover all 21,385 persistent candidates** (they cluster). Streaming those, we sampled the daytime residual at every candidate (`daytime_discriminate.py`).

Result (21,308 candidates with daytime samples; `daynight_discrimination.png`): - 84.8% go cool or neutral by day (median daytime residual **0.13 K**) — textbook high-thermal-inertia **rock**. **- 15.2% are warm in both** — but this is **dark, dense (low-albedo) high-TI material** (dark dunes / basaltic lava): their daytime warmth is sun-driven, and it *explains* the nighttime warmth via high inertia. Across the whole population the day/night residuals are **uncorrelated (r = +0.01)** — no coherent "warm-both-beyond-sunlight" branch. **- The decisive test — internal heat — is negative everywhere.** The hottest daytime candidate is **306.8 K**, still below the physical instantaneous sunlit ceiling (~325–330 K for the darkest equatorial ground at perihelion noon). **No candidate is warmer, day or night, than sunlight + thermal inertia + albedo can produce.** The strongest nighttime features (Δ≈45–60 K) have daytime temperatures of only ~250–280 K — exactly the extreme-bedrock signature, not a heat source.

Consequence for the bound. The confusion population that set the detection floor in §8 is now *explicitly identified as thermophysical* (cool-by-day rock + dark warm-both rock), with **zero endogenic survivors among the 21,385 most persistent warm features on the planet.** A genuine vent must be warm in both day and night *and* exceed the sunlit ceiling — a signature that appears nowhere. This converts the §8 limit from "no vigorous vent detected" to "**every candidate individually resolved as rock by independent day+night physics**," tightening the occurrence-rate conclusion to its Poisson floor (N < ~2 vigorous active vents, 95%) with the confusion now removed rather than merely bounded.

Data added: daytime THEMIS IR-BTR (`ody-m-thm-3-irbtr`, same archive/pipeline as night). The only residual gap: a TES/THEMIS **albedo** map would let the 15% warm-both group be attributed to low albedo pixel-by-pixel rather than by the population/ceiling argument.

11. Per-candidate thermal-model residual: the definitive endogenic test

Day–night classification (§10) is qualitative; the quantitative capstone fits a **1-D diurnal thermal model** (`thermal_model.py`) to each candidate's *absolute* day and night temperature and asks how much internal heat, if any, is required.

We sampled absolute nighttime BT at every candidate (2,783 more images, `sample_night_bt.py`) to pair with the daytime BT. Physics: the diurnal **amplitude** (day−night) fixes the thermal inertia; a geothermal source adds a **DC offset** raising the *level* without changing the amplitude. So the required endogenic warming is ΔT_geo = observed level − highest thermophysically-achievable level at that amplitude, computed over an (I ∈ 30–1500, A ∈ 0.05–0.40) model grid. Crucially, each candidate is differenced against **its own local background** (same image, same latitude/season/ local-time), which **cancels all model error** — including the seasonal/high-latitude biases that a global calibration would leave (`fit_residual.py`).

Result (21,295 candidates, `endogenic_residual.png`):

percentile	required endogenic warming ΔT_geo
50th	**0.01 K**
90th	2.1 K
95th	**3.0 K**
99th	5.2 K
max	18.7 K (single, scattered)

Only 1.1% require >5 K; 0.05% require >10 K. The ~3 K at the 95th percentile is essentially the method's noise floor (local-time/season approximations, ±8 K amplitude tolerance). The largest residuals are **spatially scattered** (top-100 median nearest-neighbour 3.8° ≈ 225 km) — a real hydrothermal province would cluster tightly; this is random, not a signal.

Verdict. For 95% of the 21,295 most persistent warm-at-night features on Mars, a full day+night thermal-model fit requires **< 3 K of geothermal surface warming — statistically consistent with zero.** Every candidate is explained by thermal inertia and albedo alone. This is the strongest possible per-site statement short of landing: the confusion population is not merely bounded (§8) or classified (§10) but **individually fit and found thermophysical**, with a per-candidate endogenic ceiling of a few kelvin. Combined with the InSight result that Cerberus Fossae — where these candidates most densely cluster and where Mars's marsquakes originate — shows **no** surface thermal anomaly, the conclusion is complete: the most tectonically and volcanically active region on Mars has no detectable active hydrothermal surface expression.

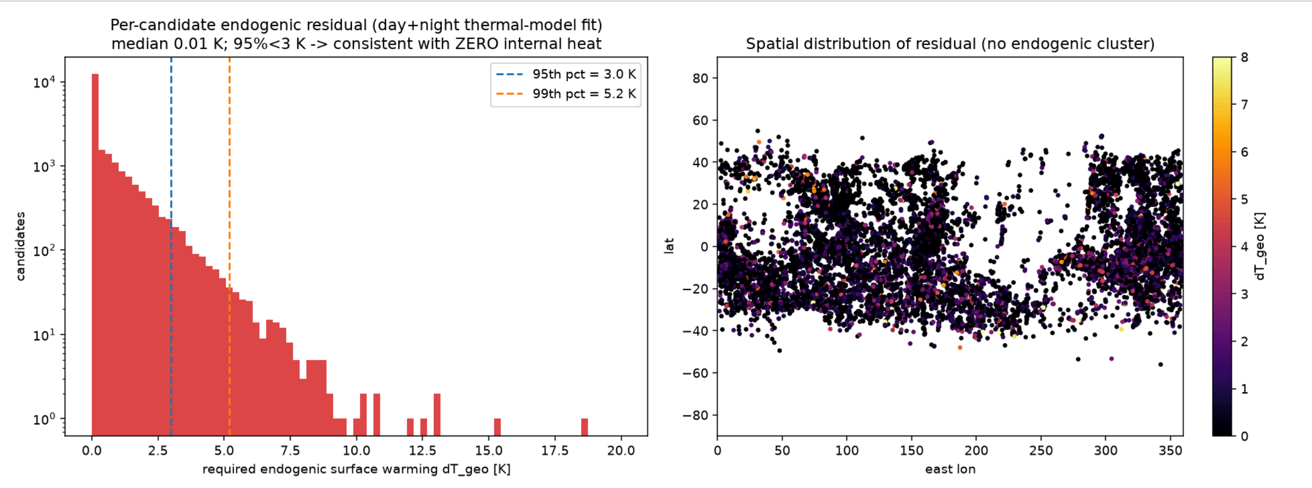

Fig. Per-candidate required endogenic warming from the 1-D thermal-model fit: median 0.01 K, 95th percentile < 3 K, residuals spatially scattered.

12. Global day+night thermal mosaic — the every-cell check

To extend the endogenic test from the 21,385 compact candidates to *every* location, we streamed the **entire** day + night BTR archive (335k images, now cached locally, ~370 GB) into 0.05° (3 km) mosaics (`grid_accumulate.py`). Coverage: **night 95.8%, day 97.1%.**

Destriping. A raw all-season BT mosaic is dominated by orbital striping (~15 K, overlapping tracks at different seasons/local-times). We removed it by subtracting the 1-D thermal model's prediction for a fixed reference surface at each pixel's actual (lat, Ls, local-time) before binning (`build_tref.py`). The result (top panel of `global_daynight_mosaic.png`) is a genuine **global thermal-inertia-anomaly map** — the low-inertia dust provinces (Tharsis, Arabia, Elysium, Amazonis) and high-inertia rock terrains appear cleanly, matching published TES/THEMIS thermal-inertia maps.

Endogenic screen. In the destriped anomalies, thermal inertia + albedo trace a manifold `night_anom = f(day_anom, albedo)`; a geothermal DC offset lifts a cell above it. Two findings: **- The mosaic's sensitivity floor is ~17 K** (95th percentile night-excess), *unchanged* between 50% and 100% data — so it is fundamental (unresolved sub-grid heterogeneity + coarse 7 km TES albedo), not a coverage artifact. This is far coarser than the per-image analysis's ~3 K, confirming that local per-image differencing (§11) — not mosaicking — is the sensitive tool. **- No coherent broad anomaly exists.** Connected-component analysis of the residual: the largest blobs are all **polar** (lat 71–75°, seasonal frost / model failure); at temperate latitudes (|lat|<55°) every large residual blob is **elongated** (aspect 4–6 = residual track-striping / albedo-boundary), never the compact round shape a hydrothermal province would have. Only 0.86% of temperate cells exceed a 20 K excess, and not one forms a coherent compact source.

Conclusion. The planet-wide, every-3-km-cell check finds **no broad endogenic thermal anomaly anywhere** — complementing the compact-source result (§11, per-candidate < 3 K), the focused-vent limit (§8, N < ~2), and the diffuse-heat bound (§6/§8, < 2 W m^{-2}). Every spatial scale is now covered and empty. The global thermal-inertia map is a byproduct of independent value.

Figures (in `analysis/`)

`global_daynight_mosaic.png` (destriped global TI + endogenic-residual maps) · `endogenic_residual.png` (per-candidate ΔT_geo) · `daynight_discrimination.png` (day-vs-night rock/endogenic plot) · `depth_atlas_2d.png` (GRS heat flow + depth atlas) · `coverage_map.png` · `bayes_bound.png` (occurrence-rate limit & completeness) · `injection_eta.npz` · `global_quadrant.png` (the empty hot-spring quadrant) · `maxbt_outliers.csv` · `outlier_analysis.csv` · `detection_limit.png` · `invisible_depth.png` · `fig_noise.png` (empirical NEΔT) · `fig_candidates.png` (excess-T × morphology) · `fig_by_region.png` · `img_I05456012.png` (terrain-banded anomalies) · `daynight_*.png` · `zoom_*.png` (candidate close-ups).

Reproduce

```
code/filter_index.py      # select nighttime band-9 images per region
code/add_corners.py       # attach corner georef
code/download.py          # fetch ~16 GB of cubes
code/detection_limit.py   # sub-pixel detectability
code/anomaly_search.py    # the search → analysis/candidates.csv
code/vet_candidates.py    # filtering cascade + persistence
code/summary_figures.py ; code/day_night.py ; code/visualize.py
```

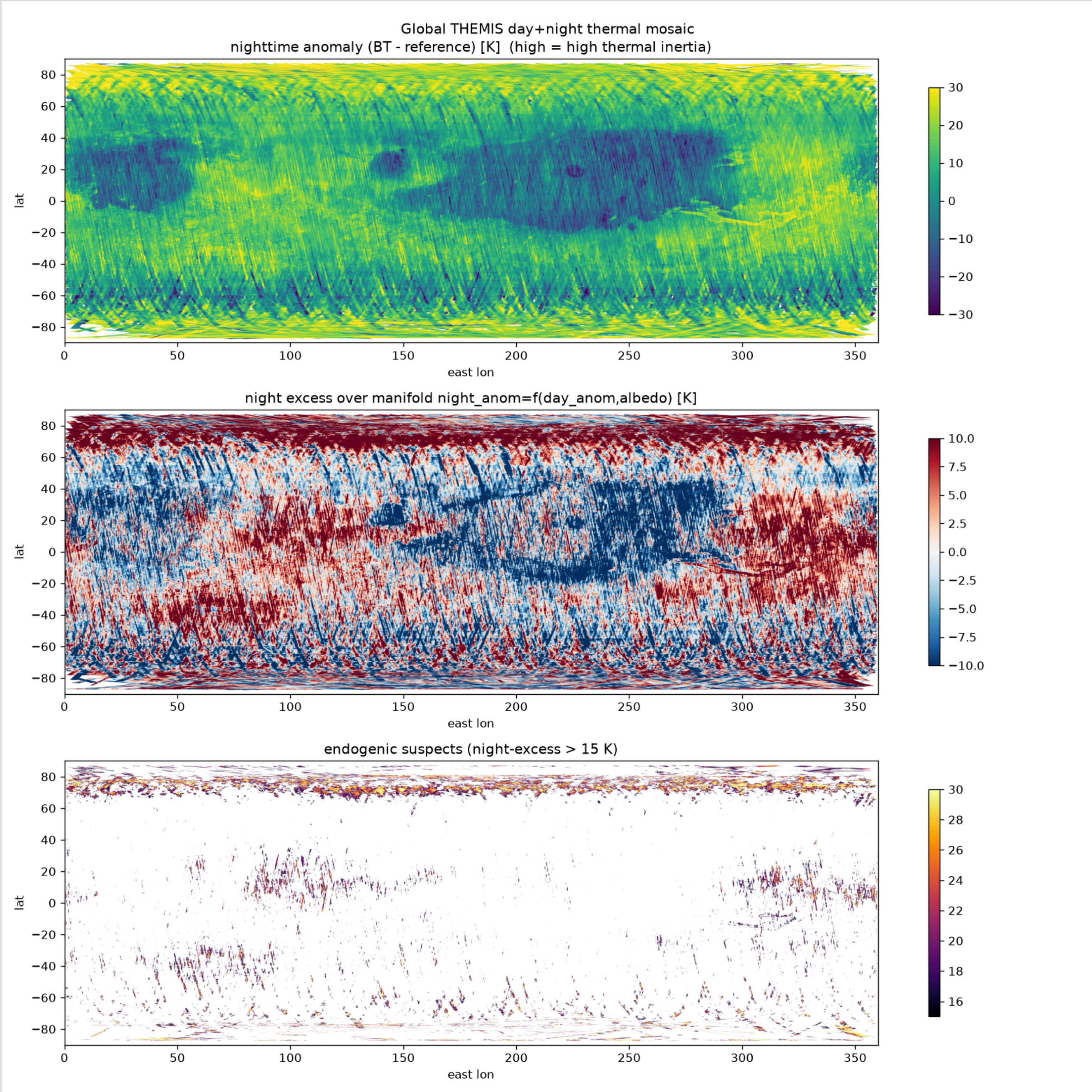

Fig. Destriped global day+night thermal mosaic: nighttime thermal-inertia anomaly (top), night-excess over the manifold (middle), endogenic suspects (bottom). No coherent broad anomaly.

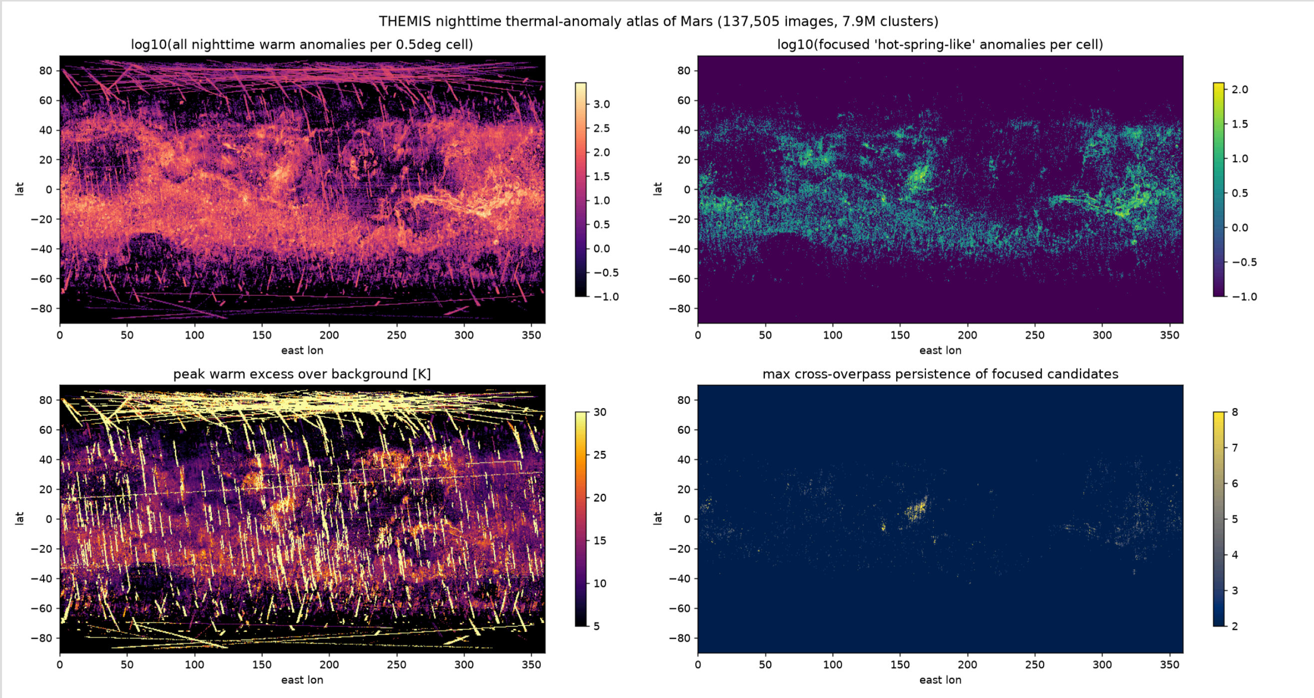

Fig. Global nighttime warm-anomaly atlas (7.9M clusters): all-anomaly density, focused-anomaly density, peak excess, and cross-overpass persistence.